

Sep.2016 / Vol.155

M i t s u b i s h i E l e c t r i c

# ADVANCE

Power Devices

• **Editorial-Chief**

*Kiyoshi Sakai*

• **Editorial Advisors**

*Toshio Masujima*

*Kotaro Aiba*

*Hiroshi Takenaka*

*Hiroaki Sakai*

*Eiji Taniguchi*

*Chikao Nishida*

*Hitoshi Suzuki*

*Kunihiko Egawa*

*Shinichi Kuroda*

*Tadashi Kato*

*Hiroaki Imamura*

*Hideyuki Takasago*

*Noboru Shirakura*

*Takayuki Hayashi*

*Toshihiro Kurita*

• **Vol. 155 Feature Articles Editor**

*Junji Yamada*

• **Editorial Inquiries**

*Kiyoshi Sakai*

Corporate Total Productivity Management

& Environmental Programs

Fax: +81-3-3218-2465

• **Product Inquiries**

**America**

*Tony Sibik*

Powerex, Inc.

173 Pavilion Lane

Youngwood, PA 15697-1800, USA

Marketing

Fax: +1-724-925-4393

Web: [www.pwr.com](http://www.pwr.com)

**Europe**

*Robert Wiatr*

Mitsubishi Electric Europe, B.V.

German Branch

Gothaer Strasse 8, 40880 Ratingen,

Germany

Power device marketing

Fax: +49-2102-486-3670

**China**

*Qian Yu Feng*

Mitsubishi Electric & Electronics (Shanghai)  
Co., Ltd.

29F, Shanghai Maxdo Centre

No.8, XingYi Road, ChangNing, Shanghai,

P.R.C.

Marketing

Fax: +86-21-5208-1502

**Mitsubishi Electric Advance** is published on line quarterly (in March, June, September, and December) by Mitsubishi Electric Corporation. Copyright © 2016 by Mitsubishi Electric Corporation; all rights reserved. Printed in Japan.

The company names and product names described herein are the trademarks or registered trademarks of the respective companies.

## CONTENTS

### Technical Reports

Overview .....1  
by *Akihiro Shima*

7th Generation Power Chip Technologies for Industrial Application .....2  
by *Ryu Kamibaba* and *Noboru Morimoto*

Packaging Technology for Highly Reliable Industrial Power Modules .....6  
by *Shinsuke Asada* and *Hiroshi Yoshida*

7th Generation IGBT Module "T Series" for Industrial Applications .....10  
by *Masaomi Miyazawa* and *Kota Ohara*

7th Generation IPM "G1 Series" for Industrial Applications ....14  
by *Yoshitaka Kimura* and *Takehiro Araki*

All-in-One Type DIPIPM with Built-In Converter, Inverter and Brake .....18  
by *Kosuke Yamaguchi* and *Tomofumi Tanaka*

### Precis

The number of applications of power devices as the central part of equipment that uses power electronics (PE) is growing. Mitsubishi Electric, which is constantly striving to develop power modules with cutting-edge chips and packages for new products, is working to meet market needs for PE equipment. This issue covers Mitsubishi Electric's latest power module technologies and trends.

# Overview



Author: Akihiro Shima\*

## Latest Trends and Prospects for Power Module Technology

Power electronics (PE) is a core technology that allows efficient utilization of electric energy, which is an urgent issue. At the heart of PE equipment are power devices, and the performance of a power device effectively determines the performance of the PE equipment. At Mitsubishi Electric, Si (silicon)-IGBT (Insulated Gate Bipolar Transistor) chips, which control high current density by conductivity modulation of bipolar devices are used in combination with module package technology, allowing us to offer a lineup of power module products ranging from over 100 watt class to several megawatt class. With this lineup, we provide high performance PE equipment in the fields of consumer products, industries, automobiles, electric railway, and electric power.

Along with the expansion of applications, the diversification in user demands for power modules. In response, we are actively introducing not only the latest 7th generation Si chip technology and SiC (silicon carbide) device technology to reduce the loss of energy but also high-density package technology to realize smaller, lighter modules. We are improving electromagnetic interference performance on modules and moreover, enhancing their functionality.

We will strive to help create highly reliable and efficient industrial equipment, offering for industrial use advantageous power modules characterized by high quality, low energy loss, excellent noise performance, and simple assembly for the benefit of users.

# 7th Generation Power Chip Technologies for Industrial Application

Authors: *Ryu Kamibaba\** and *Noboru Morimoto\**

The enhancement of properties toward low loss, low radiation noise, wide safe operating area (SOA), and high reliability is demanded of Si power devices considering the increasing range of application. The present Si power devices, on which much research has been conducted, are approaching their limit in terms of physical properties. However, we believe that there is still room to enhance the value of Si power devices through sophisticated design that allows such measures as optimization for specific uses and improvement in usability. With the aim of reducing steady-state loss and switching loss in insulated-gate bipolar transistors (IGBTs) and diodes, Mitsubishi Electric has made efforts to evolve IGBTs to planar type, trench type, and carrier-stored trench-gate bipolar transistor (CSTBT) type IGBTs. For diodes, we have evolved diffusion wafer diodes to thin wafer diodes.

This article describes our successful initiative to improve the existing technologies, and to develop 7th generation IGBTs and diodes as IGBT modules for industrial use.

## 1. 7th Generation IGBTs

### 1.1 Enhancement of IGBT performance

From the 5th generation IGBTs, we started using trench-gate IGBTs in our own CSTBT<sup>(1)</sup> structure in which a carrier-stored layer (CS layer) is formed. The CS layer allowed a significant reduction in the junction field-effect transistor (JFET) resistance, which constitutes the highest resistance in a cell. For the 6th generation, we narrowed the trench-gate pitch, thereby enhancing the carrier storing effect. The 7th generation successfully attained high performance and high drive controllability through ultra-thin wafer processing and improvement in the MOS and backside structure.

The performance of an IGBT is discussed in terms of the figure of merit (FOM)<sup>(2)</sup>. This is a numerical value expressed by Equation (1) using the values of the collector current density  $J_c$  (A/cm<sup>2</sup>), the saturation voltage between the collector and emitter  $V_{CEsat}$  (V), and the turn-off switching loss  $E_{off}$  (mJ/A).

$$FOM = \frac{J_c}{V_{CEsat} \times E_{off}} \quad \dots\dots\dots (1)$$

While the FOM of a 5th generation IGBT is 1 in a 1,200 V IGBT for industrial use, the FOM of the 6th and 7th generation IGBT is 1.25 and 1.32, respectively. We have thus succeeded in upgrading the performance for each new generation. In addition, we have taken various measures for improving the MOS and backside structures and shrinking the termination structure in response to the demand for low cost, operability under high temperature, high SOA capability, and other properties.

### 1.2 Features of the 7th generation IGBT structure for industrial use

Figure 1 shows a schematic cross-sectional view of a 7th generation IGBT for industrial use together with its features. The 7th generation IGBT has a light punch-through (LPT) structure formed by using ultra-thin wafer processing technology, thereby reducing the loss. While the thin wafer process is effective for improving electrical properties, there have been issues such as a reduction in SOA capability due to decreased heat capacity of the chip and variations in electrical properties caused by mechanical stress. The 7th generation 1,200 V IGBTs for industrial use have secured the current capability and SOA capability through optimization of the area ratio between the n<sup>+</sup> emitter layer and p<sup>+</sup> layer in the MOSFET. Secondly, a

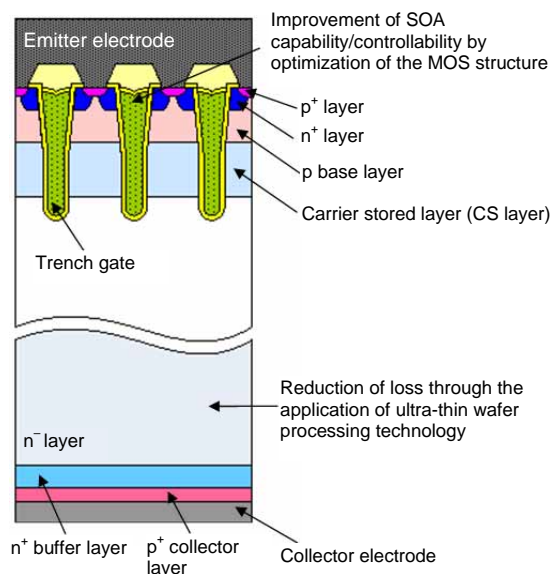


Fig. 1 Cross-sectional view of the structure of a 7th generation IGBT for industrial use and its features

stress relief processing technology for the thin wafer that does not impose mechanical stress on the chips has been developed through optimization of the processing conditions in the grinding and thermal process, etc. Furthermore, as a result of optimizing the gate capacitance (between the gate emitter and collector) by adjusting the ratio between the active and non-active states of the trench gate in 7th generation IGBTs, the current dependence of the reverse recovery  $dv/dt$  (hereafter referred to as “ $dv/dt$ ”) when turning on has been improved, thus realizing high  $dv/dt$  controllability.

### 1.3 Electrical properties of a 7th generation IGBT for industrial use

Figure 2 shows the waveform of the short-circuit safe operating area (SCSOA) of a 7th generation IGBT for the use of industrial IGBT modules. Thinning of a wafer reduces the thermal capacitance, which causes a decline in the SCSOA. However, the saturated current  $I_{sat}$  (voltage between the gate and emitter ( $V_{GE}$ ) = 14 V, temperature at the connection ( $T_j$ ) = 150°C; rated current  $\times 2$ ) and the latch-up endurance ( $T_j$  = 175°C; rated current  $\times 2$ ) have been retained through optimization of the area ratio between the  $n^+$  emitter layer and  $p^+$  layer. As a result, the 7th generation IGBT remained unbroken during measurement up to the pulse width of 10.5  $\mu s$ , under measuring conditions of  $V_{CE}$  = 800 V,  $V_{GE}$  = 15 V/–15 V, and  $T_j$  = 150°C, thus achieving the current capacity and high SOA capability that satisfy the product requirements.

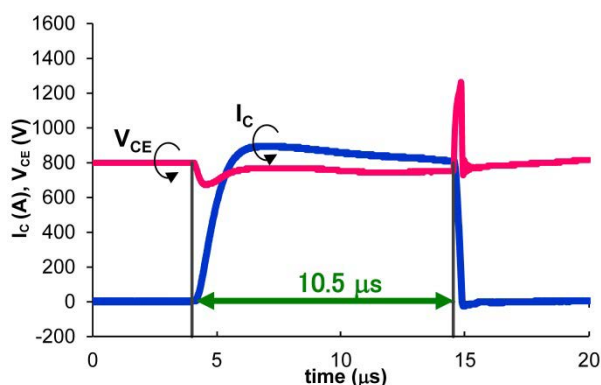


Fig. 2 SCSOA waveform of a 7th generation IGBT

Moreover, wafer thinning may cause mechanical stress that is imposed on a chip and causes the properties to fluctuate, which makes the stress relief during wafer processing very important. It was the key to focus particularly on the processing conditions for the grinding, electrode formation, and thermal processing as the optimization to realize an ultra-thin wafer process not only for small-capacity chips but also for large-capacity chips.

Figure 3 shows surface photographs of a

small-capacity chip with a rated voltage of 600 V and rated current of 20 A, and a large-capacity chip with a rated voltage of 650 V and rated current of 200 A using ultra-thin wafers, and the in-plane variation of the threshold voltage  $V_{GE(th)}$  between the gate and emitter.<sup>(3)</sup> The area of the chip in Fig. 3(b) is approximately 20 times that in Fig. 3(a). The threshold voltage ( $V_{GE(th)}$ ) of MOSFET portion is characterized by the carrier mobility, which is sensitively affected by the mechanical stress. For this reason, the in-plane variation of  $V_{GE(th)}$  is useful as an index for confirming the mechanical stress caused by warpage of the chip. Figure 3(c) and (d) shows the difference in variation of wafer in-plane  $V_{GE(th)}$ . In-plane variation  $V_{GE(th)}$  in each case does not exceed  $\pm 0.2$  V, showing no significant difference between (c) and (d). This suggests that the wafer was thinned without the excessive stress to cause the fluctuation of the characteristic.

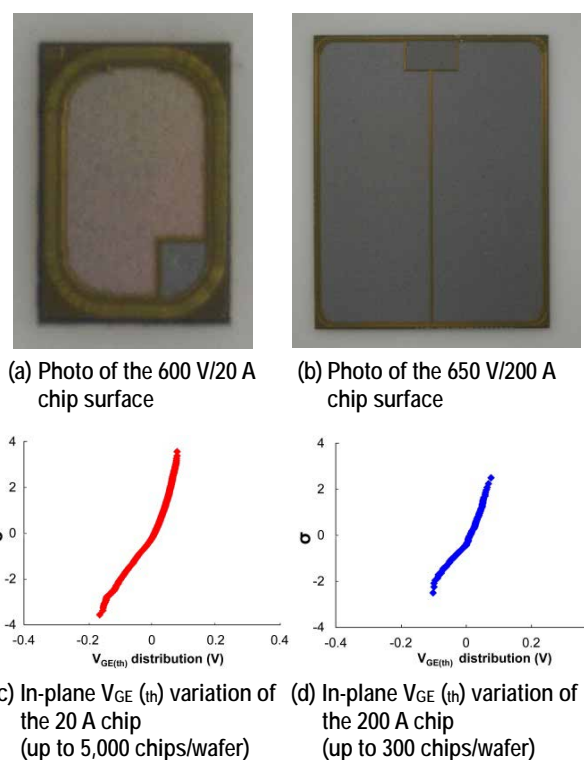


Fig. 3 Photos of the surface and in-plane homogeneity of the 7th generation chip

The next topic is the controllability of the 7th generation IGBTs with the optimized gate capacitance. IGBTs are basically turned on and off by charging or discharging through the gate voltage applied between the gate and emitter. This gate switching at high frequencies allows highly efficient control of the electrical power in case of the PWM (Pulse Width Modulation) circuit. The gate charge  $Q_g$  stands for an integral of the MOS channel current and time period of turn-on, so it also corresponds to the capacitance coming from the depletion layer built by the reverse bias across the main

junction; the emitter and collector. So the rate control easiness of this voltage raising and descending of  $dv/dt$  are preferable from the users' point of view. When this  $dv/dt$  exceeds the reference value (e.g., 20 kV/ $\mu$ s), radiation noise is generated, leading to malfunction in a motor, etc. For this reason, the gate resistance  $R_{g(on)}$  is adjusted to a value large enough to reduce the  $dv/dt$  so as not to exceed the reference value in the current range used. On the other hand, when the  $dv/dt$  is too small compared to the reference value, the switching will be slow. This causes the switching energy  $E_{on}$  to increase when turning on. Accordingly, the current dependence of  $dv/dt$  is preferable to be as small as possible along the entire current range of usage.

Figure 4 shows the diode's reverse recovery  $dv/dt$  during IGBT's turn-on dependency of the 6th generation and 7th generation IGBTs on the collector current  $I_c$ . Both IGBTs use a chip with a rated voltage of 1,200 V and rated current of 110 A, under switching conditions of  $V_{CE} = 600$  V,  $V_{GE} = 15$  V/-15 V,  $T_j = 25^\circ\text{C}$ , gate resistance  $R_{g(on/off)} = 10\ \Omega$ , and the collector current in a range of 5 to 110 A is allocated. The  $dv/dt$  value of the 6th generation IGBT when  $I_c = 5$  A is increased by about 2.2 times when  $I_c$  is 110 A. On the other hand, the  $dv/dt$  of the 7th generation IGBT when  $I_c = 5$  A is increased by about 1.6 times when  $I_c$  is 110 A, showing the ability to maintain an almost constant switching speed in the allocated current range. As described above, optimization of the gate capacitance has improved controllability for the  $dv/dt$  of the 7th generation IGBT.

## 2. 7th Generation Diode

### 2.1 Enhancement of diode performance

An effective means for enhancing the performance of a diode is reduction of the forward drop voltage  $V_F$  by making the wafer thinner. However, reducing chip thickness increases the risk of destruction due to high voltage peak (snap-off) during the reverse recovery, i.e.,

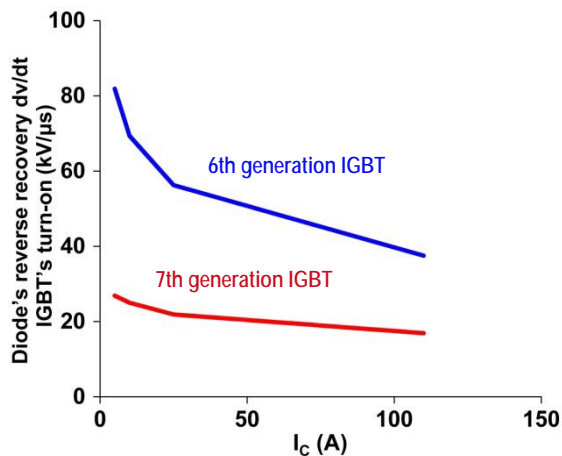


Fig. 4 Comparison of the reverse recovery  $dv/dt$ - $I_c$  characteristics between 6th and 7th generation IGBTs

the SOA degradation. To solve this problem, we have developed RFC diodes adopting a new backside structure technology. In the RFC diode structure, a p layer is partially formed on the cathode side and holes are injected from the p layer avoiding a carrier-empty state during reverse recovery action. As a result, the electric field on the cathode side is relaxed and the snap-off voltage is suppressed.

To date, we have applied the RFC diode structure, in addition to the thinned wafer, to our 7th generation diodes of 1,200 V class or above.<sup>(4)(5)</sup> The following sections present the results of trial manufacture and evaluation of a 650 V 7th generation diode for industrial use.

### 2.2 Features of the 7th generation (RFC) diode structure

Figure 5 shows the cross-sectional structure of a conventional diffusion wafer diode and a 7th generation diode. The thickness of the 650 V 7th generation diode has been reduced to about one-third of the thickness of the conventional diffusion wafer diode by means of ultra-thin wafer processing technology. Furthermore, an  $n^+$  cathode layer/p layer structure has been formed on the backside through a backside patterning process.

### 2.3 Electrical properties of 7th generation diodes

Figure 6 shows the reverse recovery waveform of a 7th generation diode chip. It is reported that the oscillation phenomenon becomes significant under conditions of high power-supply voltage ( $V_{cc}$ ), high wiring inductance ( $L_s$ ), low operation temperature, and other factors of hard recovery. To optimize the RFC diode parameters, we conducted the evaluation using the chip with a rated voltage of 650 V and rated current of 100 A under conditions in which the oscillation

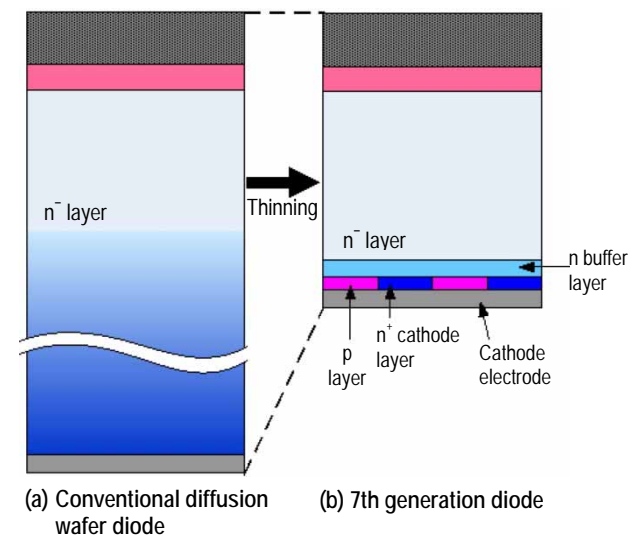


Fig. 5 Comparison between schematic cross-sectional views of conventional and 7th generation diodes



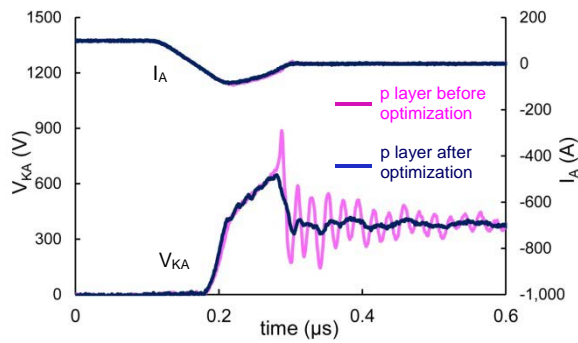


Fig. 6 Reverse recovery waveform of 7th generation diodes under conditions in which the oscillation phenomenon is prone to occur ( $V_{cc}=400V$ ,  $I_A=100A$ ,  $T_j=25^\circ C$ )

phenomenon was likely to occur. As described above, hole injection from the p layer on the backside produces a moderate reverse recovery waveform (soft recovery) for an RFC diode. This means that adjusting the concentration and layout of the p layer in accordance with the wafer thickness and usage conditions allows control of the hole injection.

The snap-off of voltage and subsequent oscillation were observed with the chip prior to the optimization of conditions. However, optimization of the parameters made it possible to suppress the snap-off so as not to exceed 650 V, thus achieving SOA capability equivalent to that of the conventional diode.

Thanks to the RFC structure, the 7th generation diode has better tradeoff relationship between  $V_F$  and  $E_{rec}$  than the conventional diffusion wafer diode, as shown in Figure 7. Accordingly, with the 7th generation diodes, we reduced  $E_{rec}$  by 30% with the same  $V_F$  comparing to the conventional diffusion wafer diode. In addition, the FOM of the 7th generation diode, which can be expressed by Equation (2), was increased by 50%.

$$FOM = \frac{J_A}{V_F \times E_{rec}} \quad \dots\dots\dots (2)$$

$J_A$ : Anode current density (A/cm<sup>2</sup>)

$V_F$ : Forward direction voltage drop at 125°C (V)

$E_{rec}$ : Reverse recovery loss at 125°C (J/A per pulse)

As described above, the 7th generation diodes with the low loss but the wide SOA capability are suitable to a wide variety of conditions for industrial use.

### 3. Conclusion

Focusing on the improvement of usability for industrial use, we have developed 7th generation IGBTs and diodes with high performance and high SOA capability through the new technologies such as

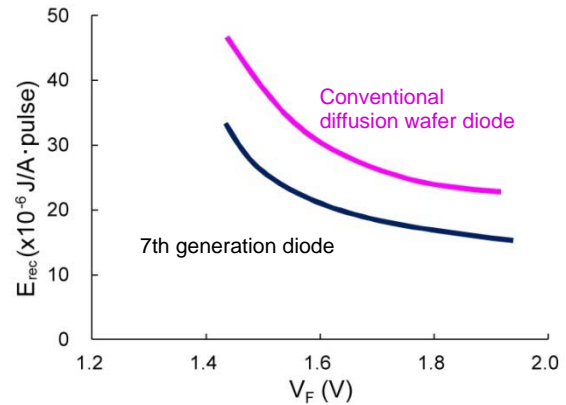


Fig. 7  $V_F$ - $E_{rec}$  trade-off relationship of conventional and 7th generation diodes ( $V_{cc} = 300V$ ; forward direction current  $I_F = 100A$ ;  $T_j = 125^\circ C$ )

ultra-thin wafer processing and the backside doping profile designing. As a result, we succeeded in realizing 7th generation IGBTs with the higher controllability of  $dv/dt$  through optimization of the MOS structure, and with suppression of oscillation through optimization of the backside structure.

The ultra-thin wafer processing technology has been used for IGBTs and diodes of 600 V to 1,400 V. In addition, this backside designing of diodes are also applied to the entire voltage classes up to 6,500 V. Going forward, we will strive to develop 8th generation Si power chips with enhanced performance, controllability, and quality in response to market demands.

### References

- (1) Takahashi, H., et al.: Carrier Stored Trench-Gate Bipolar Transistor (CSTBT) – A Novel Power Device for High Voltage Application, ISPSD1996, 349–352 (1996)
- (2) Sato, K., et al.: New chip design technology for next generation power module, Proceedings of PCIM 2008, 673–678 (2008)
- (3) Kamibaba, R., et al.: Next Generation 650V CSTBT with improved SOA fabricated by an Advanced Thin Wafer Technology, ISPSD2015, 29–32 (2015)
- (4) Masuoka, F., et al.: Great Impact of RFC Technology on Fast Recovery Diode towards 600V for Low Loss and High Dynamic Ruggedness, ISPSD2012, 373–376 (2012)
- (5) Suzuki, K., et al.: High Performance and Wide SOA Capability 7th Generation Power Chip Technology, Mitsubishi Denki Giho, 88, No. 5, 281–284 (2014).

# Packaging Technology for Highly Reliable Industrial Power Modules

Authors: Shinsuke Asada\* and Hiroshi Yoshida\*

## 1. Introduction

In the field of industrial equipment, power modules have an extensive range of applications that includes not only motor control units, but also equipment for uninterruptible power supplies and conversion of power generated from natural energy, and their use continues to increase in line with the demand for saving energy. This trend is driving the need for industrial power modules that are more reliable and easier to install. To meet these needs, we have developed the 7th generation IGBT module T series NX type for industrial use. This article describes the features and reliability of the package structure of the product.

## 2. Packaging Technology for Improved Reliability

### 2.1 Concept of package design

Figure 1 shows the appearance of the newly developed module. To increase the reliability, we revised many of the package components. As shown in Fig. 2(a), the conventional package has a structure in which a ceramic substrate is soldered to a copper baseplate. However, in this type of structure, when the temperature of the module changes due to the external environment, heat generated by turning on the power, or other factors, the difference in the coefficient of thermal expansion between the copper baseplate and ceramic substrate produces stress on the solder layer. Accordingly, the module needed to be designed to prolong the service life. The new package structure, as shown in Fig. 2(b), features a newly developed (1) insulated metal baseplate and (2) direct potting encapsulation, which alleviates the stress caused by heat within the module.



Fig. 1 Appearance of the developed module

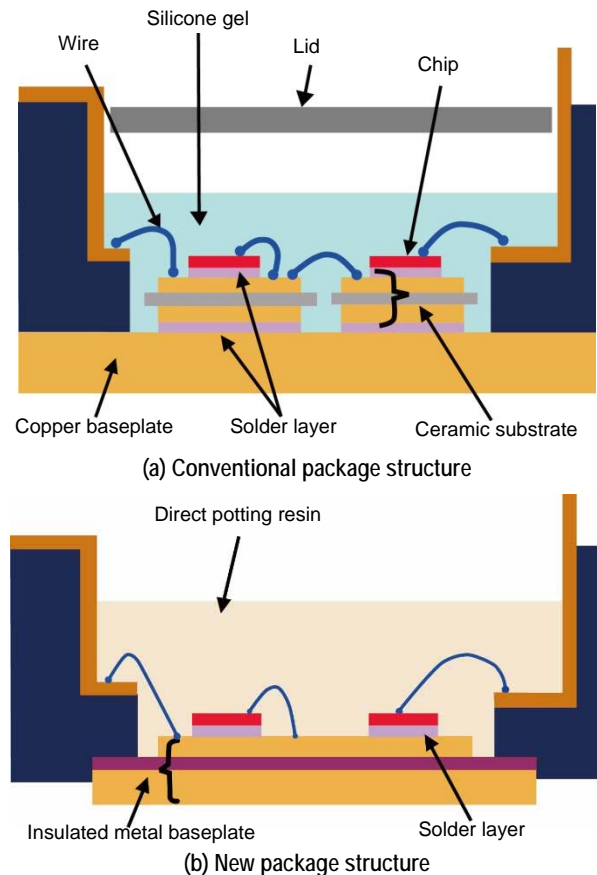


Fig. 2 Comparison between the cross sections of package structures

### 2.2 Insulated metal baseplate

The newly developed module adopts an insulated metal baseplate, which has the conventional functions of both the ceramic substrate for wiring and insulation and the copper baseplate for thermal diffusion. The insulated metal baseplate is a substrate with a resin insulation layer and wiring patterns directly formed on a copper baseplate. We designed the package structure without the ceramic substrate used in the conventional structure, in order to reduce the thermal stress induced by the mismatch between the two coefficients of thermal expansion. In addition, the required insulation and heat dissipation properties are secured by adopting a material with high thermal conductivity for the resin insulation layer.



### 2.3 Direct potting encapsulation

Mitsubishi Electric has already commercialized a transfer molded structure<sup>(1)</sup> that provides a service life several times longer than the silicone gel encapsulation structure prevailing in power modules. Taking advantage of this, we developed a direct potting encapsulation technology with the aim of applying hard resin encapsulation similar to encapsulation using a mold resin to the case structure of the package for industrial use. Unlike transfer molding in which a solid resin is used, a liquid resin material was developed, allowing encapsulation by injecting liquid resin into the case structure. Furthermore, by matching the coefficients of thermal expansion, the thermal stress acting on the solder under the chip and wires inside the package has been reduced.

### 2.4 Simplification of the assembling process

In the assembling process of a module with the conventional structure, it is necessary to assemble the ceramic substrate and copper baseplate, which are prepared separately. However, in the new structure, these two components have been integrated into the insulated metal baseplate, thus reducing the number of assembling parts and soldered joints. This further simplifies the assembling process compared to the conventional structure, eliminating the factors that cause variations in the manufacturing quality.

### 2.5 Reliability in endurance to heat cycles

Figure 3 shows the results of a heat cycle test ( $-40^{\circ}\text{C} \leftrightarrow 125^{\circ}\text{C}$ ), comparing scanning acoustic tomography (SAT) images taken in the vicinity of a substrate corner with the conventional and new package structures, in the initial state and the state after applying the same number of heat cycles. In the conventional structure, slight cracks can be seen in the solder joint layer under the ceramic substrate, whereas in the new structure without a solder joint layer, no abnormality is observed. In addition, we also confirmed that there was almost no influence from thermal stress on the solder layer under the chip after applying the

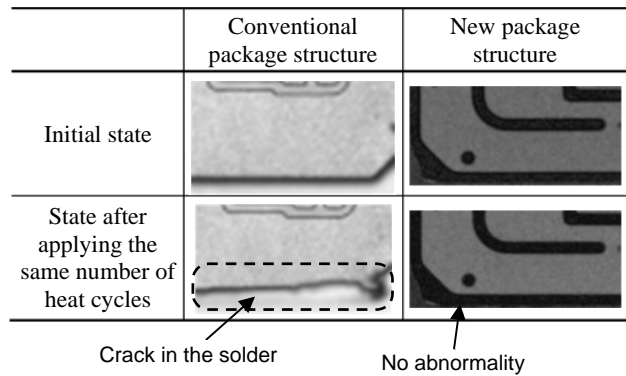


Fig. 3 Comparison of SAT images after heat cycle test

same number of heat cycles. As shown in Fig. 4, we think that this is attributable to the reduction in stress at the solder joints as a result of matching the coefficient of thermal expansion of the direct potting resin with that of the insulated metal baseplate.

## 3. Packaging Technology for Simplified Installation

### 3.1 Concept for simplification of installation

As shown in Fig. 5, power modules for industrial use are generally set up with the external terminals connected to a printed circuit board. In addition, heat sinks are attached to the back of the module to release heat, and a thermal interface material (TIM) is provided between the module and heat sink to facilitate the heat release. In the conventional structure, it is necessary for users to solder the external terminals to a printed circuit board, as well as apply grease as a TIM, before attaching the heat sink to the module. To simplify these processes, we also made a power module that comes with pressfit terminals and a phase change thermal interface material (PC-TIM) available for users.

### 3.2 Pressfit terminals

The pressfit connection uses a contact load to produce an electrical connection between a printed circuit board and the terminals. A pressfit terminal slightly larger than the diameter of the through-hole on

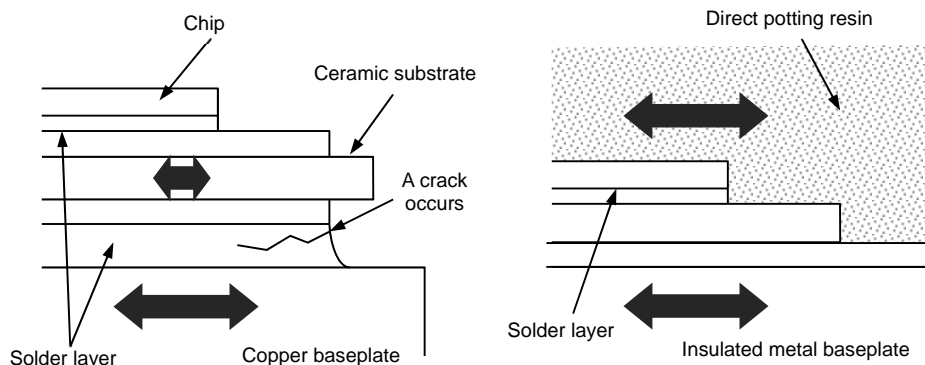


Fig. 4 Schematic cross-sectional view showing the method for improving the reliability

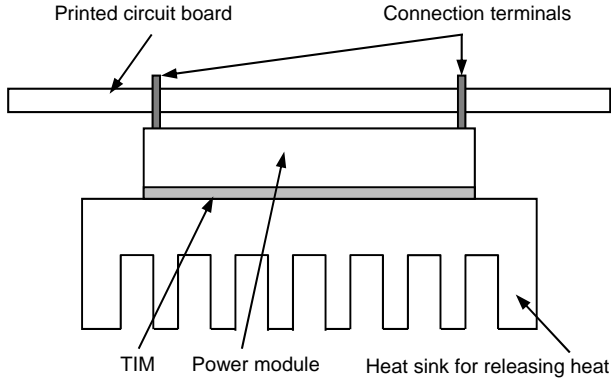


Fig. 5 Assembled structure of the module

a printed circuit board is pressed into the through-hole, thereby providing a contact load (Fig. 6). We have applied this technology to the connection terminals of power modules. By using the power module with pressfit terminals, all the terminals can be connected to a printed circuit board at once just by setting the power module and the printed circuit board and pressing. Thus, the process of assembling a module to a printed circuit board is simpler than the conventional assembling process by soldering.

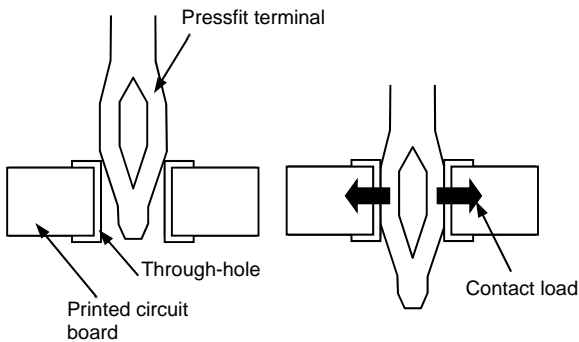


Fig. 6 Pressfit technology

### 3.3 PC-TIM (phase change thermal interface material)

Unlike conventional heat conductive grease, the PC-TIM is in a solid state at approx. 45°C or below, and liquefies at above 45°C. These characteristics can be used to store and transport power modules printed with the PC-TIM, which means that the PC-TIM can be put on power modules as part of the manufacturing process. This enabled the installation process to be simplified further, by eliminating the need to apply heat conductive grease which is conventionally required.

When a power module using the PC-TIM is pressed against a heat sink for releasing heat, the PC-TIM does not spread thinly, unlike the case of heat conductive grease. When the PC-TIM starts to soften

after the temperature exceeds approx. 45°C, the material stretches in the lateral direction under the influence of clamping pressure, until it becomes thick in the wide gaps between the power module and heat sink, and thin in the narrow gaps, regardless of the shape of the object being clamped. The PC-TIM entering the gaps pushes out the air between the power module and heat sink. Figure 7 is a photograph of the appearance of a module with the PC-TIM printed in a hexagon pattern. This pattern was selected given the wetting extendability of the PC-TIM. Figure 8 shows the results of a test in which the wetting expansion of the PC-TIM was observed using a transparent board instead of a heat sink. It was confirmed that the wetting expanded over the entire face of the base without any gaps. Figure 9 compares the thermal resistances ( $R_{th(j-t)}$ ) of two different TIM materials. The application of the PC-TIM with high heat-release properties reduces the heat resistance by approx. 20% compared with general heat conductive grease.

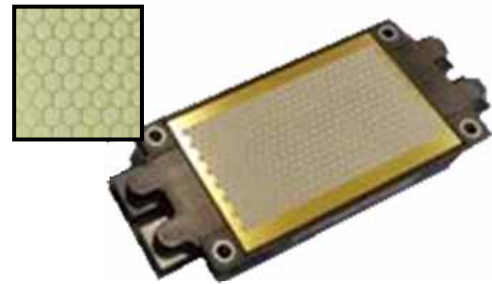


Fig. 7 Image of the module with the PC-TIM applied



Fig. 8 Image of the spread PC-TIM

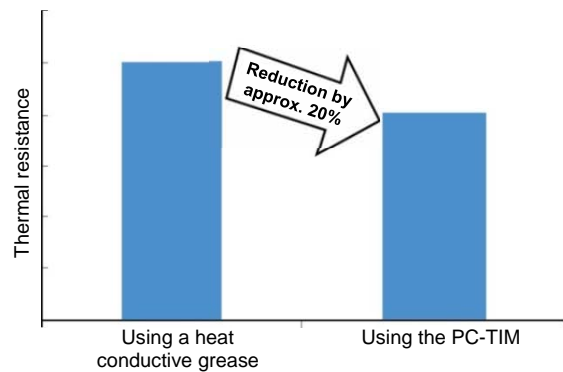


Fig. 9 Comparison between the simulated thermal resistance values

#### 4. Conclusion

The high reliability of the newly developed 7th generation IGBT module T series NX type for industrial use has been achieved through the combined application of the insulated metal baseplate and direct potting encapsulation, which was adopted after re-examining the component parts used in the conventional package structure. Furthermore, we offer an optional version that comes with pressfit terminals and PC-TIM that makes it easy to install the module to the user's system. This new module will help create an energy-saving society and satisfy the needs of users.

#### Reference

- (1) Shinohara, T., et al.: High Current Transfer-Molded Power Module, Mitsubishi Denki Giho, 81, No. 5, 325–328 (2007).

# 7th Generation IGBT Module “T Series” for Industrial Applications

Authors: Masaomi Miyazawa\* and Kota Ohara\*

## 1. Introduction

IGBT modules for industrial are characterized by low loss and high reliability and are used in a wide range of applied equipment in the industrial market, including inverters, servo amplifiers, wind power generation, solar photovoltaic generation, and UPSs. In recent years, IGBT module is required higher reliability and the reduction of power consumption in order to achieve enhanced energy efficiency and longer life time. To meet this demand, we have newly developed the 7th generation IGBT module named “T series” which consists of a new structure and 7th generation chips. This paper describes the features and characteristics of the “NX type package” (Fig. 1) and “std type package” (Fig. 2) of the 7th generation IGBT modules.



Fig. 1 NX type package (62×152 mm)



Fig. 2 std type package (62×108 mm)

## 2. Features of the 7th Generation T Series

### 2.1 Reduction of power loss

Loss simulation in the case of PWM inverter operation was performed under the condition that conventional and proposed IGBT modules have the same level of radiation noise. As shown in Fig. 3, the total loss of 7th generation IGBT module is reduced by approximately 10% in comparison with 6th generation IGBT module.

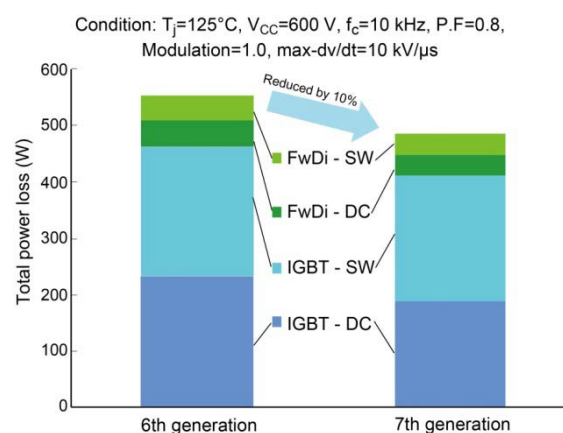


Fig. 3 Results of loss simulation of 1,200 V/450 A

### 2.2 High reliability

The case temperature  $T_c$  of an IGBT module varies greatly due to the start and stop operations of a system. As the module is composed of multiple materials, thermal expansion by the difference in the coefficient causes considerable stress at each material boundary, resulting in fatigue in a thermal cycle test to simulate this behavior,  $T_c$  is changed by repeatedly turning on and off the power, thereby enabling assessment of the product life time. Figure 4 shows the 6th generation structure<sup>(1)</sup>, 7th generation NX type structure<sup>(2)</sup>, and 7th generation std type structure<sup>(3)</sup>. With the 6th generation structure, as solder is fragile compared to copper and ceramics, a crack in the solder layer under the substrate where the stress is especially high is one of the factor to decide life time. On the other hand, in the 7th generation structure in which the insulation part and the copper base are combined, the solder layer under the substrate has been eliminated, therefore it becomes possible to enhance the thermal cycle capability.

Figure 5 shows the scanning acoustic tomograph (SAT) images of the 6th generation structure and 7th generation NX type package structure in the initial state and the state after applying the same number of heat cycles. In the 6th generation structure, a crack can be seen in the solder layer under the ceramic substrate, whereas in the 7th generation structure without a solder layer, no deterioration is observed in the resin layer of the insulated metal baseplate.

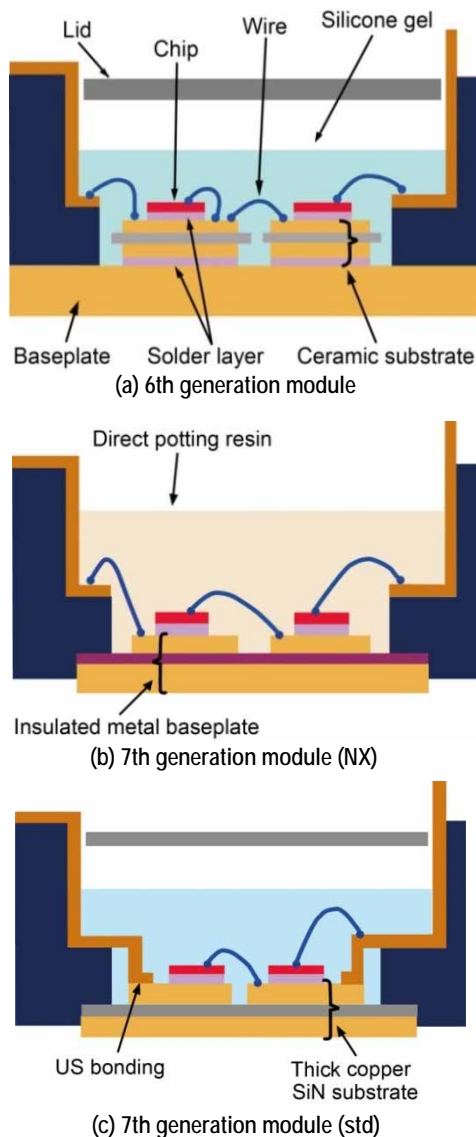


Fig. 4 Comparison of the structure between the 6th generation module, 7th generation module (NX), and 7th generation std type package

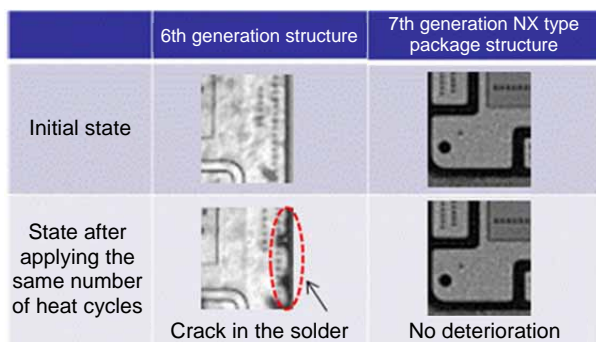


Fig. 5 Comparison of SAT images after a thermal cycle test

### 2.3 Product lineup

Table 1 shows the T series lineup. A total of 48 models of the 650 V and 1,200 V NX type packages (soldered terminals/pressfit terminals) and std type

packages have been newly developed as our 7th generation IGBT module. The connection to a printed circuit board using the pressfit terminals can be completed by setting and pressing the module. It is a simple process for users in comparison with the conventional soldering connection. As the models with pressfit terminals are added to the NX type packages, users can choose either the conventional terminals to be soldered or the pressfit terminals. Added to the standard type package is a 1,200 V/600 A model, commercialized for the first time, with external dimensions of W62 × D108 mm. In addition, optional application of the PC-TIM (phase change thermal interface material) is available with all 48 models. PC-TIM-applied products enable to reduce the coating process in users, therefore it is easier to handle than when thermal grease is used.

Table 1 Lineup

Package type	Model name	Rated voltage	Rated current	Circuit configuration	External dimensions W×D (mm)
NX type solder pin package + pressfit package	CM300DX-13T	650V	300A	2in1	62×152
	CM300DXP-13T		450A		
	CM450DX-13T		600A		
	CM450DXP-13T		100A	6in1	62×122
	CM600DX-13T		150A		
	CM600DXP-13T		200A		
	CM100TX-13T	1,200V	150A	7in1	62×137
	CM100TXP-13T		200A		
	CM150TX-13T		225A	2in1	62×152
	CM150TXP-13T		300A		
	CM200TX-13T		450A		
	CM200TXP-13T		600A	6in1	62×122
	CM150RX-13T		1000A		
	CM150RXP-13T		100A		
	CM150TX-24T		150A	7in1	62×137
	CM150TXP-24T		200A		
	CM200RX-13T		150A		
	CM200RXP-13T		100A	2in1	34×94
Standard type package	CM100DY-13T	650V	150A		
	CM150DY-13T		200A	2in1	48×94
	CM200DY-13T		300A		
	CM300DY-13T		400A		
	CM400DY-13T		600A	2in1	62×108
	CM600DY-13T		100A		
	CM100DY-24T	1,200V	150A		
	CM150DY-24T		200A	2in1	34×94
	CM200DY-24T		300A		
	CM300DY-24T		450A		
	CM450DY-24T		600A	2in1	48×94
	CM600DY-24T		100A		



### 3. Package

#### 3.1 NX type package

The structure of the 7th generation NX type package greatly changed from conventional 6th generation package structure. The 6th generation structure is composed of a ceramic substrate, copper baseplate and solder under the chips and substrates as the materials under the chips. As shown in Fig. 2(b), 7th generation NX type package structure has newly adopted an insulated metal baseplate equipped with insulation part and copper base part. The insulated metal baseplate by using a copper baseplate, thick copper foil layer and an insulated resin sheet optimized for its heat dissipation and insulating performance. Moreover, optimization of the thickness of the copper base part and patterns has reduced the mass by 15% of that of compared with the 6th generation package. As shown in Fig. 4(a), (b), in contrast to the multiple substrates used in the 6th generation structure, the 7th generation NX type package structure has one unified the insulated metal baseplate.

As a result, wires used for electrically connecting substrates are no longer needed, thus reducing the internal inductance by 30% in comparison with the 6th generation (1,200 V/300 A model).

Conventional 6th generation IGBT module used gel to cover chips and bonding wires above a substrate.

The 7th generation NX type package structure adopts newly developed direct potting resin that is optimized for reducing mechanical stress.

#### 3.2 Std type package

Next, we describe the features of the thick copper SiN (silicon nitride) substrate in the 7th generation standard type package in which the substrate and the copper baseplate are combined. The thick copper SiN substrate is a ceramic substrate as with a conventional AlN (aluminum nitride) substrate, but differs from the AlN substrate in the copper pattern thickness and the material/thickness of the insulation layer. We tripled the conventional thickness of the copper pattern on the chip side, thereby increasing the thermal diffusion before the heat passes through the insulation layer, which is disadvantageous in terms of heat conduction. Also, the tripled copper pattern thickness allows the passage of a large current with a narrower circuit pattern width. The change in the insulation layer material from AlN to Si<sub>3</sub>N<sub>4</sub> has increased the mechanical strength of the substrate, allowing an increase in the substrate dimensions as well as the thinned insulation layer, and ensuring the high reliability of the US bonding. The thickened copper pattern and the expanded substrate size eliminates the use of the conventional wires between substrates, making it possible to increase the chip mounting area,

and to optimally arrange a large current circuit pattern. Thanks to these benefits, the 7th generation std type package series comes with high-capacity chips in a smaller package that is compatible with a conventional sized package.

### 4. Chip

#### 4.1 7th generation IGBTs

Figure 6 shows the schematic cross-sectional view of a 7th generation IGBT. For the 7th generation IGBTs, we used our CSTBT (carrier stored trench-gate bipolar transistor) structure as with the 6th generation IGBTs. The wafer thickness has been reduced by approx. 10%, thereby improving the trade-off between the collector-emitter saturation voltage  $V_{CEsat}$  and turn-off switching loss  $E_{off}$  (Fig. 7). SOA capability with thin chips is secured through the optimization the area ratio between the n<sup>+</sup> emitter layer and p<sup>+</sup> layer in the MOSFET. By optimizing the gate capacitance, improving the controllability of the reverse recovery dv/dt through the gate resistance  $R_G$ . In other words,  $R_G$  smaller than that of a conventional IGBT module lowers the reverse

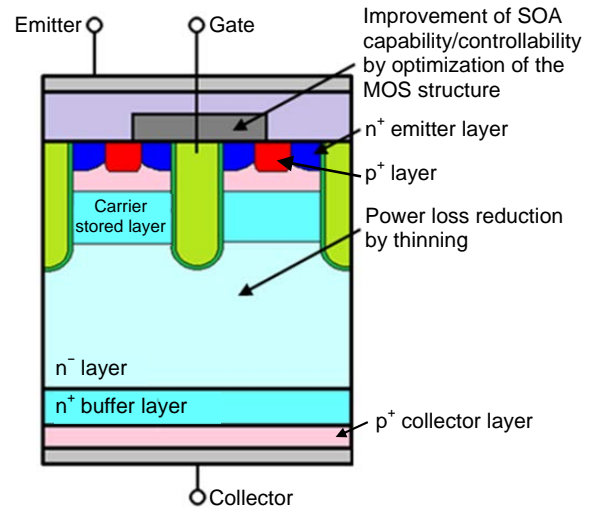


Fig. 6 Cross-sectional view of the 7th generation IGBT chip

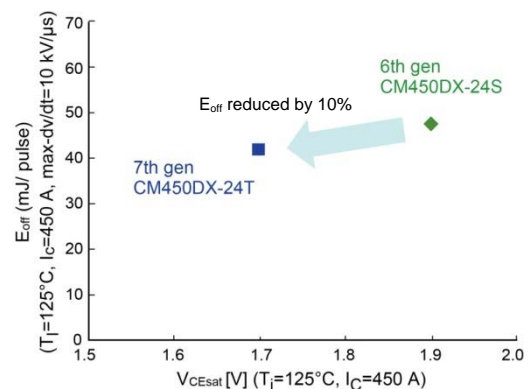


Fig. 7 Comparison of the  $V_{CEsat}$ - $E_{off}$  trade-off



recovery  $dv/dt$ , reducing the turn-on switching loss  $E_{on}$  by 10% at the same  $dv/dt$  (Fig. 8).

## 4.2 7th generation diodes

Figure 9 shows the schematic cross-sectional view of a 7th generation diode. For the 7th generation diodes, which are RFC (Relaxed Field of Cathode) diodes with a structure containing  $p^+/n^+$  layers formed at the cathode using the technology for backside dopant profiling, the wafer thickness has been reduced by approx. 20% compared with a 6th generation diode. This RFC diode made it possible to reduce the wafer thickness while suppressing the oscillation which is an

issue when thinning a wafer, thereby improving the trade-off between the emitter-collector voltage  $V_{EC}$  and the reverse recovery loss  $E_{rr}$  compared to a conventional diode (Fig. 10).

## 5. Conclusion

In the 7th generation IGBT modules, as we introduced a new structure for the package in which the insulation part and copper base part are integrated, and adopted the 7th generation chips, our new product has low power loss and high reliability. Furthermore, our lineup has been added with the NX type package models and standard type package models, offering the option of using the PC-TIM for all models and meets the needs of users. Going forward, we will develop 7th generation IGBT modules in the market to contribute to an energy-saving society.

## References

- (1) Nishiyama, T., et al.: 6th Generation IGBT Module "NX Series," Mitsubishi Denki Giho, 84, No. 4, 240–243 (2010).
- (2) Ohara, K., et. al.: A New IGBT Module with Insulated Metal Baseplate (IMB) and 7th Generation Chips, PCIM Europe 2015, 1145–1148 (2015)
- (3) Miyazawa, M., et al.: 7th Generation IGBT Module for Industrial Applications, PCIM Europe 2014, 34–38 (2014)

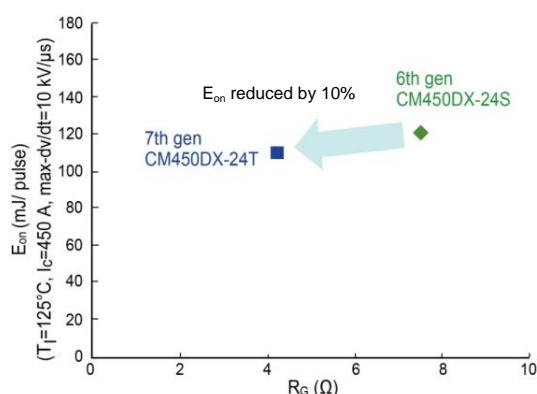


Fig. 8 Comparison of the  $R_G$ - $E_{on}$  trade-off

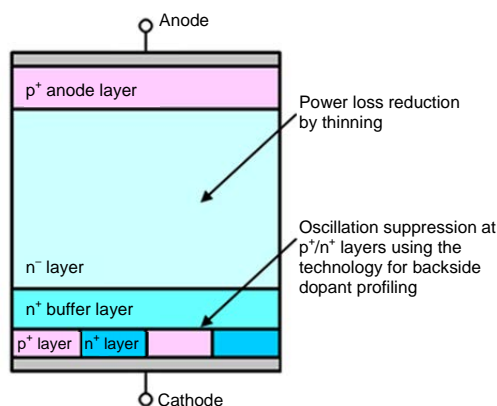


Fig. 9 Cross-sectional view of the 7th generation diode chip

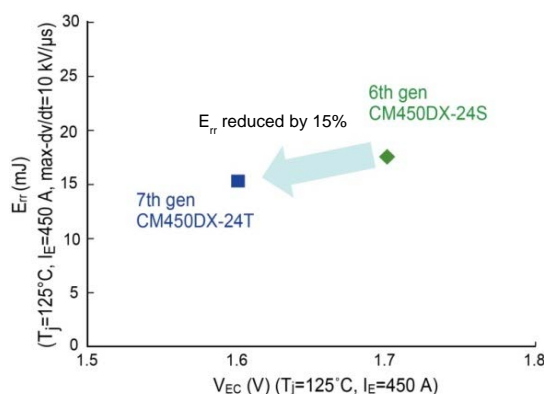


Fig. 10 Comparison of the  $V_{EC}$ - $E_{rr}$  trade-off

# 7th Generation IPM “G1 Series” for Industrial Applications

Authors: Yoshitaka Kimura\* and Takehiro Araki\*\*

This paper introduces the “G1 series” 7th generation IPMs for industrial applications. The G1 series IPMs, which use 7th generation IGBT chips, feature a new package structure as well as a newly designed external shape for improved ease of use. The IPMs also realize a power loss reduction function for the overload region, made possible through the use of a low-noise IGBT drive circuit.

## 1. Introduction

Given the recent trend toward energy efficient equipment for global environmental conservation, there is an increase in demand for power semiconductor devices, which are indispensable for high-power conversion. In particular, IPMs (Intelligent Power Modules) have a built-in drive circuit and protective circuit, so IPMs users are unnecessary to design these circuit. Such characteristics are attractive to those seeking easy-to-use power modules. In addition, as users increasingly prefer modules that allow more efficient design of the housing, there is a need for power module to consider assemblability. Moreover, in the inverter system market in which industrial IPMs are prevalent, there is a high demand for smaller, lighter products and expanded product lineups.

The extensive lineup of the G1 series IPMs is characterized by light weight and high reliability thanks to a structure that uses an insulated metal baseplate, and a low-noise IGBT drive circuit that reduces the power loss. The specifications of the modules were developed in pursuit of user friendliness.

## 2. Outline of the G1 Series IPMs

### 2.1 Product lineup

The G1 series IPMs mounted with 7th generation power chips constitute a new product lineup. Three different types of packages are available depending on the Voltage/Current rating of the product, as shown in Table 1. The lineup consists of products with rated current from 50 A to 450 A at 650 V rated voltage, and from 25 A to 200 A at 1,200 V rated voltage.

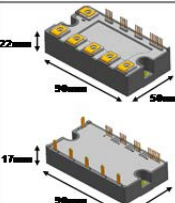
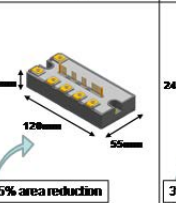
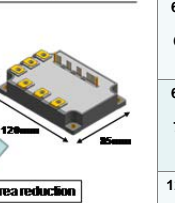
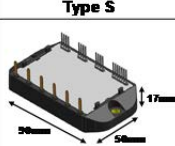

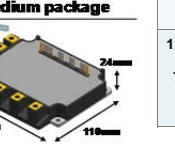
Moreover, given the demand for product downsizing and expanded lineups, there is a clear need for packages with a narrower width or smaller dimensions in order to downsize the housing in which multiple power modules are often mounted. The packages of the G1 series IPMs have a smaller width and dimensions than those of the L1 series IPMs. The mounting area of the B-package is 25% smaller than L1 series IPM with the same rated voltage/current, and that of the C-package is 31% smaller than L1 series IPM. Therefore, G1 series IPMs contribute to miniaturization and weight reduction of the inverter device.

Figure 1 shows the lineup of the G1 series IPMs. As these three package types offer products with common ratings, users can select a package suitable for the intended use.

### 2.2 Features of A-package

The G1 series A-package modules offer two types of main terminal specifications: the solder pin type and the screw type. The mounting areas are same in both

Table 1 Package specifications of the G1/L1 series IPMs

	Package Outline		
	A-pkge	B-pkge	C-pkge
G1 series			
		25% area reduction	31% area reduction
L1 series	Type S 	Small package 	Medium package 

	Current capacity								
	25A	35A	50A	75A	100A	150A	200A	300A	450A
650V			A						
6in1			B					C	
650V			A						
7in1			B					C	
1200V			A						
6in1			B					C	
1200V			A						
7in1			B					C	

Fig. 1 Lineup of G1 series IPMs

terminal types. But these models allow users to select a main terminal type that is suitable for the mounting process or the specifications for the connection of power modules. In addition, consider a case in which multiple modules with different packages are mounted in the same housing, as shown in Fig. 2, in which the G1 series A-package and B-package modules are mounted. As the G1 series A-package modules with the screw main terminals and the B-package modules are of the same height, users can have a uniform main wiring height as shown in Fig.3. Thus, the external shape of the G1 series IPMs is designed to make the modules easy to assemble into devices.

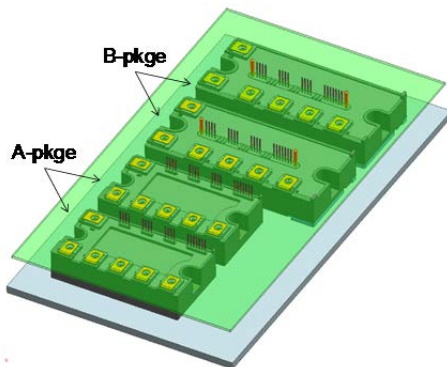


Fig. 2 Layout example of multiple IPMs

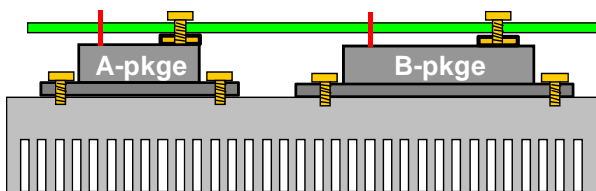


Fig. 3 Uniform height of the main wiring that connects an A-package module (with the screw main terminals) with a B-package module

### 3. Package Structure

For power modules, it is used ceramic insulating substrate from conventional in order to achieve both a high heat radiation and insulation in power module. However, for the G1 series with a goal of extending the service life, ceramic substrate has been replaced by an insulated metal baseplate to form a structure with no soldering; also, the direct potting technology has been applied using epoxy resin as the encapsulation material. Figure 4 shows the cross-sectional view (vertical structure) of an L1 series IPM and a G1 series IPM.

One of the methods for evaluating the service life of a module is thermal cycle testing. When a system is repeatedly started up and stopped, the module temperature is changed. So, thermal stress is generated in the module structural components. This causes a difference in the coefficients of thermal expansion between structural components. As a result, the deterioration (cracks) of the solder layers occur. In

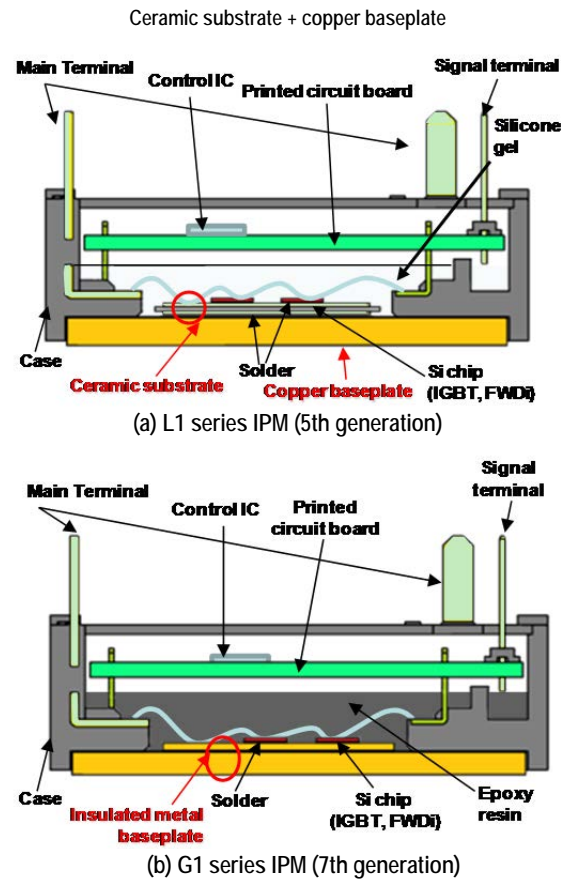


Fig. 4 Structure comparison between an L1 series IPM and a G1 series IPM

conventional IPM structures, solder is used for the bonding between the copper baseplate and ceramic substrate. In such structures, the progress of cracks in the solder layer under the insulation substrate leads to a decrease in thermal cycle resistance.<sup>(1)</sup>

The G1 series IPMs have optimized coefficients of thermal expansion of the solderless structure under the insulation substrate and encapsulation material, thereby alleviating the thermal stress imposed on the structural components. This improves the thermal cycle life, which has been caused the deterioration of the solder layer under the insulation substrate. And thus the modules have achieved high reliability.

### 4. Functions of G1 series IPMs

#### 4.1 Low-noise IGBT drive circuit

The G1 series IPMs adopt the low-noise IGBT drive circuit that is used in the L series IPMs for reducing EMI (Electro-Magnetic interface) noise. Figure 5 schematically shows the principle of the low-noise IGBT drive circuit.

Based on conventional control systems, because the  $dv/dt$  changes sharply in the low current region, EMI noise is prone to occur. However, when the  $dv/dt$  in the

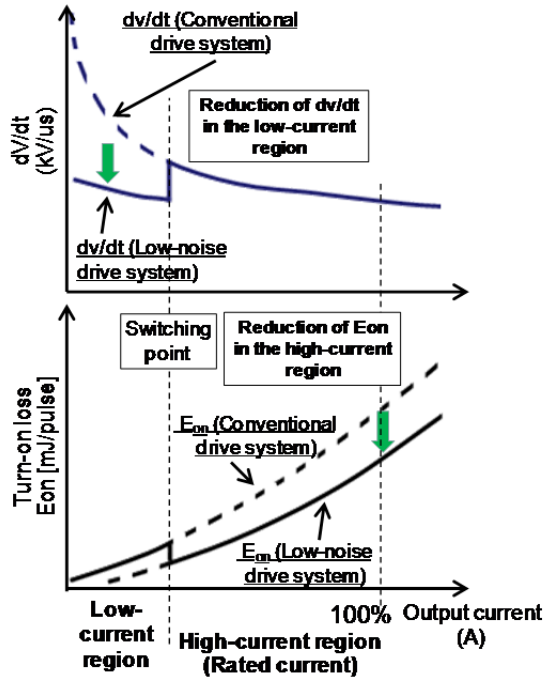


Fig. 5 Principle of the low-noise IGBT drive circuit

low-current region is reduced in order to suppress the EMI noise, the power loss increases in both the high- and low-current regions. With the adoption of the low-noise IGBT drive circuit in the G1 series, the EMI noise can be suppressed by setting a slow  $dv/dt$  in the low-current region, while the power loss can be reduced by setting a high switching speed in the high-current region (rated current). The G1 series IPMs are capable of detecting the current passing through the IGBT in real time at the control IC by elements incorporated in the IGBT chips. When the detected current reaches the threshold value, the drive power is automatically switched. The current detection using the elements in the chips allows for the switchover of the drive systems without the need for an external detection circuit.

While reducing the power loss by this function, it is possible to reduce the EMI noise. The switchover point of the switching speed has been optimally designed for users to maximize the effect of this function.

Figure 6 shows the results of an EMI noise test conducted using two samples mounted with the control substrate of a conventional drive system and the low-noise IGBT drive circuit system as used in the G1 series IPMs. These samples mount the same power chips and same wiring circuit. The values of the EMI noise show almost the same trend across all frequency domains. Figures 7 and 8 show the simulation results for the power loss of these samples during low-current operation (normal operation mode) and high-current operation (locked operation mode) respectively. In the low-current region, the power loss per module is almost equal between the two systems, while in the high-current

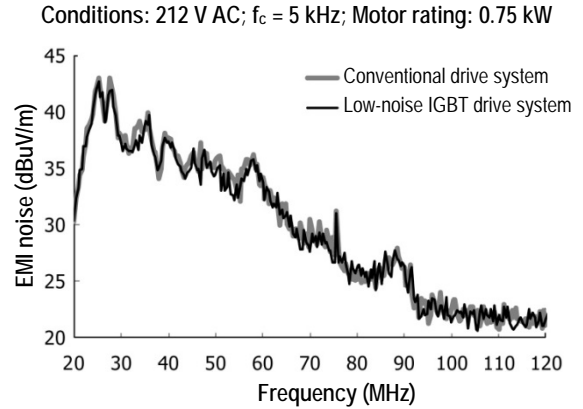


Fig. 6 Comparison of EMI (radiation) noise (G1 series IPM vs. conventional IPM)

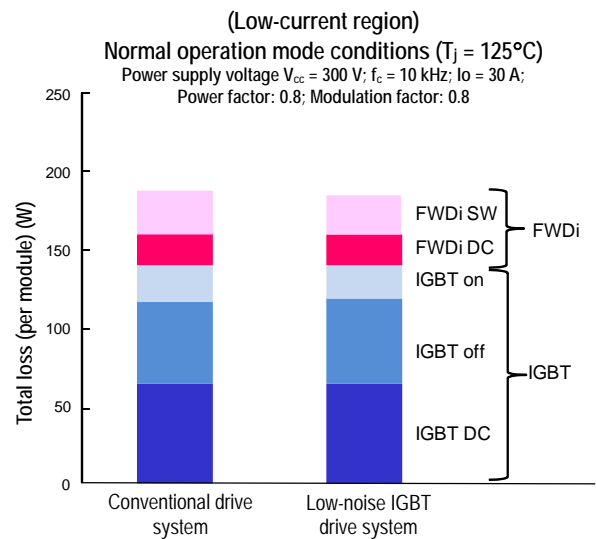


Fig. 7 Comparison of simulated power loss in the low-current region

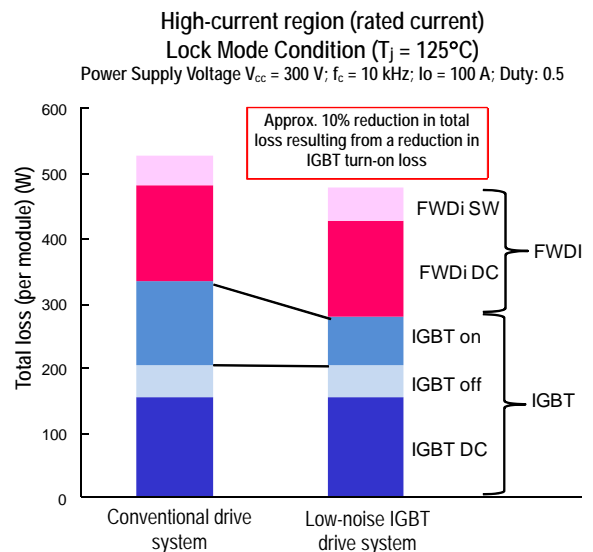


Fig. 8 Comparison of simulated power loss in the high-current region

region, the power loss of the low-noise IGBT drive circuit system module is smaller than that of the conventional drive system module. As shown in Fig. 5, a major factor in the reduced power loss is the reduction of the turn-on loss in the IGBT chips in the high-current region. By using the function of Low-noise IGBT drive circuit, it realizes an improvement of approximately 10% in the total power loss. Under the condition of the same EMI noise as the conventional drive system, this function reduces the power loss in the region of current that exceeds the switching changing point, and in particular reduces the power loss even when the motor is locked up, an unfavorable condition in terms of energy saving.

#### 4.2 Error identification function

IPMs generally have a protective circuit that turns off the IGBT in the event of an operation abnormality (increase in element temperature, occurrence of high-current, etc.). The G1 series IPMs have an error identification function in addition to the error output function in terms of conventional protective functions (over temperature [OT], under voltage [UV], and short current [SC]). The error output timing (Fo) is set for each protective function, and pulse signals are output at the specified Fo. Users can determine the details of an error when the Fo time is detected.

### 5. Conclusion

This paper introduced the product features of the new G1 series IPMs. For the new IPM packages, it is possible to make the width narrower and the total dimensions smaller compared to the packages of the L1 series IPMs. As a result, the mounting area on the B-package was reduced by 25%, and that on the C-package was reduced by 31% of the respective size counterparts in the L1 series. G1 series IPMs will help reduce the size and weight of inverter devices. In addition, the G1 series A-package IPMs offer the options of solder pin type and screw type main terminals, allowing users to select a main terminal type in accordance with the required specifications. Moreover, the same main terminal height of the A-package and B-package allows a uniform height for the main wiring, for ease of assembly by users. Furthermore, the low-noise IGBT drive circuit reduces the power loss in the overload region.

As described above, the IPMs in the extensive G1 series lineup were designed with user friendliness in mind, which includes an optimized external shape and main terminal options. The IPMs are provided with enhanced functions based on the conventional IPM products. These G1 series IPMs will satisfy diverse market needs.

### References

- (1) Ohara, K., et al. "A New IGBT Module with Insulated Metal Baseplate (IMB) and 7th Generation Chips.", PCIM Nuremberg (2015)



# All-in-One Type DIIPM with Built-In Converter, Inverter and Brake

Authors: Kosuke Yamaguchi\* and Tomofumi Tanaka\*

This paper introduces the Dual Inline Package Intelligent Power Module+ (DIIPM+) series that has been developed for all-in-one air-conditioning systems and low-capacity motor drivers of industrial general-purpose inverters, etc.

The new products come with a three-phase converter and a brake circuit in addition to the conventional DIIPM structure. Optimization of the terminal layout and the use of bootstrap diodes (BSDs) have eliminated complications in the wiring installation, and have also reduced the size and design load of the inverter system.

## 1. Introduction<sup>(1)</sup>

In 1997, Mitsubishi Electric commercialized the industry's first DIIPMs featuring a transfer molded structure with built-in power chips and control ICs. The DIIPMs have been widely used for household electrical appliances such as air-conditioners, refrigerators, and washing machines, and for industrial equipment such as all-in-one air-conditioning systems and low-capacity motor drivers. This time, with the goal of further reducing the size and design load of the inverter system, we have developed the all-in-one type DIIPM+ series in which three-phase converters and brake circuits are added to the conventional DIIPM structure. This article presents an outline and the features of the DIIPM+ series.

## 2. Outline of the DIIPM+ Series

The main circuit of the DIIPM+ consists of a three-phase AC output inverter, brake, and three-phase converter. Table 1 shows the DIIPM+ series product lineup. Figures 1 and 2 are schematic views of the internal circuit and a system using the DIIPM+, respectively.

## 2.1 Inverter

### 2.1.1 Power part

Six IGBTs and six diodes are used in the three-phase AC output inverter circuit.

### 2.1.2 Control part

One high-voltage integrated circuit (HVIC): A drive circuit for P-side insulated gate bipolar transistors (IGBTs), high voltage level shift circuit, and Under Voltage (UV) protection circuit for control power supply that does not output errors are built in. In addition, the number of terminals is reduced by combining the three-phase circuits on the P side into a chip, thereby optimizing the terminal layout and making it easy for control circuit pattern wiring.

One low-voltage integrated circuit (LVIC): A drive circuit for N-side IGBTs, Under Voltage (UV) protection circuit for control power supply, and protection circuit for short circuit are built in. The short circuit protection is performed such that the protection circuit for short circuit detects overcurrent using an externally connected shunt resistor and provides feedback to the LVIC to block IGBTs. The LVIC outputs error signals when the protection circuit for control power supply under voltage or the protection circuit for short circuit is activated. Furthermore, a function is provided to output analog signals for the internal temperature of the IPM.

Three BSDs: Bootstrap circuit diodes (with current limiting resistors) that allow for single power supply drive are provided.

## 2.2 Brake

An IGBT, diode, and driver LVIC are mounted. The LVIC has a built-in protection circuit for control power supply under voltage that does not output errors.

Table 1 DIIPM+ series product lineup

Model name	PSS05MC1FT	PSS05NC1FT*	PSS10MC1FT	PSS10NC1FT*	PSS15MC1FT	PSS15NC1FT*	PSS25MC1FT	PSS25NC1FT*	PSS35MC1FT	PSS35NC1FT*	PSS50MC1F6	PSS50NC1F6*
Rating	5A / 1200V		10A / 1200V		15A / 1200V		25A / 1200V		35A / 1200V		50A / 600V	
Application	<ul style="list-style-type: none"><li>Industrial low-capacity motor driver for general-purpose inverter and servo.</li><li>Inverter control of compressors and fan motors in industrial or package air conditioner.</li></ul>											
Main circuit components	Three-phase AC output inverter, three-phase converter circuit, brake circuit											
Built-in features	Inverter part											
	- For P-side IGBTs: Drive circuit, high pressure level shift circuit, protection circuit for control power supply voltage reduction that does not output errors, bootstrap system for single power supply drive											
	- For N-side IGBTs: Drive circuit, protection circuit for control power supply voltage reduction, short circuit protection using an externally connected shunt resistor											
	- Fo output: Error (Fo) output for the activation of the N-side IGBT protection circuit for short circuit and protection circuit for control power supply voltage reduction											
	- LVIC analogue temperature voltage output (VOT)											
Built-in features	Brake part											
	- For IGBTs: Drive circuit, protection circuit for control power supply voltage reduction that does not output errors <sup>1)</sup>											

\* Brake circuit is not included



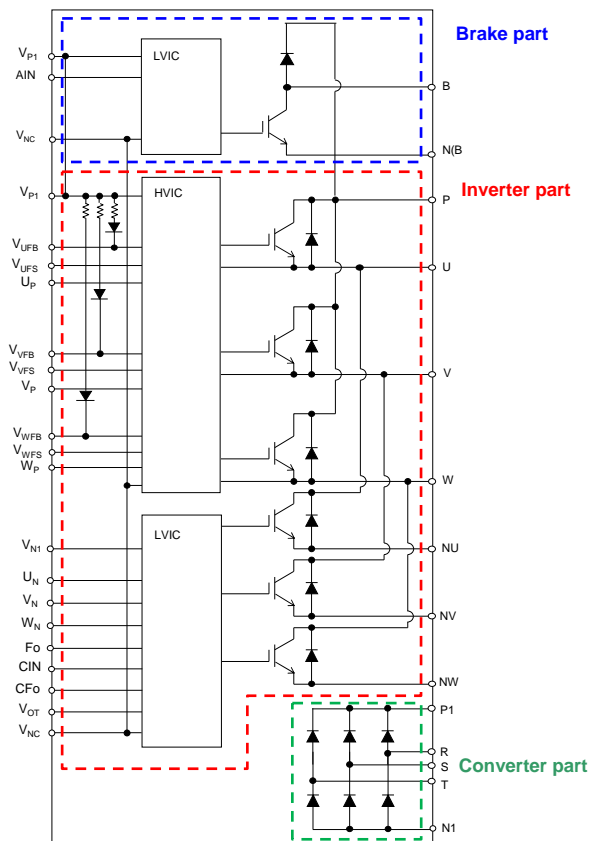


Fig. 1 Schematic view of the internal circuit

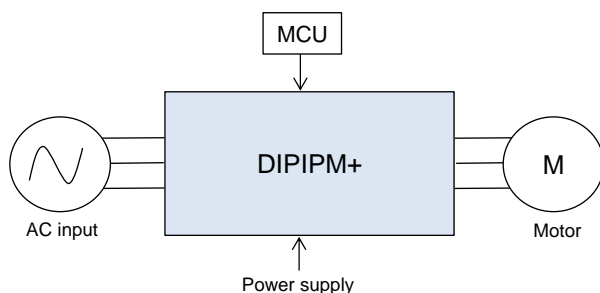


Fig. 2 Schematic view of a system using the DIIPM+

### 2.3 Converter

Six diodes are used in the three-phase converter circuit.

## 3. Features of DIIPM+

### 3.1 All-in-one structure

With the aim of realizing an all-in-one structure for the DIIPM+ series, we conserved the space for mounted circuits.

For the power part, we improved the performance of a newly developed CSTBT (carrier stored trench-gate IGBT), thereby reducing the mounted area. Regarding the control part, the conventional large DIIPM Ver. 4 series<sup>(2)</sup> has the drive IC and IGBTs connected using thin and thick wires, respectively, via lead frames. For the DIIPM+ series, combining the three-phase control ICs (HVICs) for the P-side IGBT

drive into one chip, as well as optimizing the internal pattern layout and resin flow during the shaping, made it possible to directly connect the control IC with IGBTs using thin wires, and thus downsizing the control part (Fig. 3).

These technical improvements led to an approx. 30% reduction in the area of the inverter part compared with the conventional inverter part, thereby realizing the all-in-one structure including the converter and brake parts (Fig. 4).

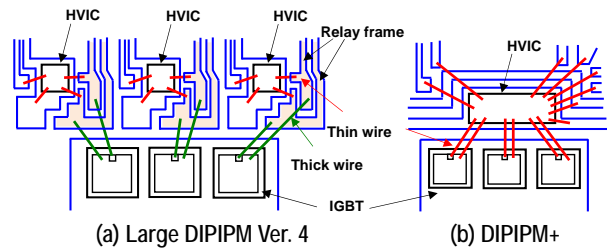


Fig. 3 Schematic internal view in the vicinity of the HVIC

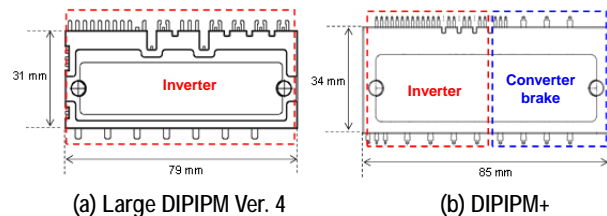


Fig. 4 Package outline

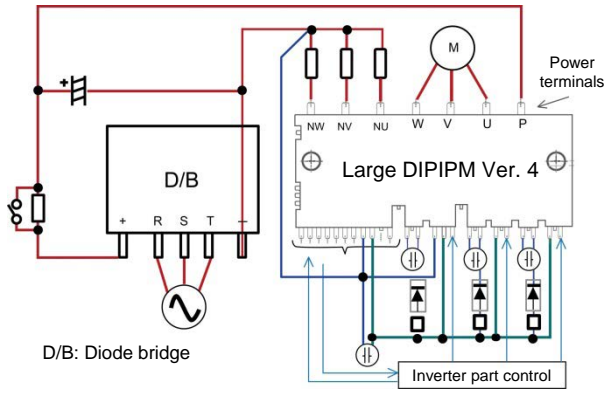
### 3.2 Designability

In the DIIPM+ series, the terminal layout has been optimized and BSDs are provided, thereby making it easy to install the wiring, and also reduce the substrate area. Figure 5 shows an example layout that uses a large DIIPM Ver. 4 and DIIPM+.

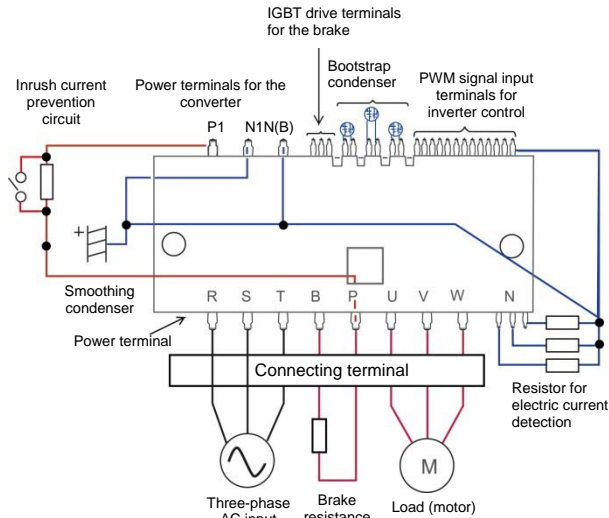
In the DIIPM+ series, the input and output power terminals for three-phase AC input, motor output, etc. are separated from the control terminals. This allows for a simple wiring design that prevents reciprocal interference between the wiring patterns. Moreover, with the built-in BSDs, single power supply drive is possible by only connecting a bootstrap capacitor, which further reduces the number of components and simplifies the wiring to decrease the PCB area.

Figure 5(b) shows the arrangement of power terminals forming a line that consists of three-phase AC input terminals (R, S, T), brake resistance connection terminals (B, P), and output terminals (U, V, W). This terminal alignment allows for direct connection to the connecting terminals of inverter equipment while installing non-intersecting wires, thereby reducing electrical surges and noise generated as a result of simplifying the wiring and reducing the PCB area.

In conformity to the wire inductance and parasitic capacitance reduced as a result of the simplification of wiring, the switching speed of IGBTs is also adjusted to



(a) Example layout that uses a large DIPIPM Ver. 4



(b) Example layout that uses a DIPIPM+

Fig. 5 Pattern layout

a low level in this series compared with the conventional products. This change reduces radiation noise, and potentially eliminates the need for a noise filtering circuit (Fig. 6). Furthermore, the maximum case temperature for operation of this series is 110°C, higher than the 100°C for conventional products, expanding the possibility of design for heat release.

The improvement from the conventional products not only reduces the direct material cost of components and the size of the PCB, but also significantly shortens the time required for design and evaluation by users.

#### 4. Performance and Features of the DIPIPM+ Series

Table 2 shows the main electrical characteristics of PSS25MC1FT (25 A/1,200 V), a representative model in the DIPIPM+ series.

This series includes a newly developed CSTBT with enhanced performance attained by applying a fine cell structure and a wafer produced using the thin wafer process technology. The structure and wafer have effectively reduced the saturated voltage  $V_{CE(sat)}$  with

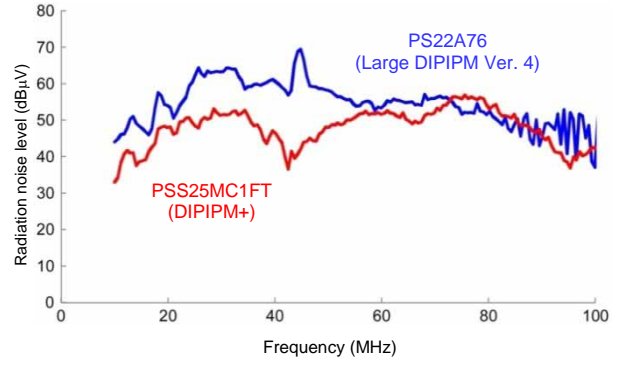


Fig. 6 Radiated noise in each frequency range (example evaluation conducted by Mitsubishi Electric)  
(Conditions:  $T_a = 25^\circ\text{C}$ ;  $V_{CC} = 600\text{ V}$ ;  $f_c = 5\text{ kHz}$ ;  $I_o = 2.5\text{ arm}$ )

Table 2 Main electrical characteristics of PSS25MC1FT (25 A/1,200 V)

##### Inverter part

Item	Condition	Minimum value	Standard value	Maximum value	Unit
$V_{CE(sat)}$	$V_D = V_{DB} = 15\text{ V}$ , $T_j = 25^\circ\text{C}$	—	1.50	2.20	V
	$V_{IN} = 5\text{ V}$ , $I_C = 25\text{ A}$ , $T_j = 125^\circ\text{C}$	—	1.80	2.45	
$V_{EC}$	$T_j = 25^\circ\text{C}$ , $-I_C = 25\text{ A}$	1.10	2.40	3.10	V
$t_{on}$	$T_j = 125^\circ\text{C}$ , $V_{CC} = 600\text{ V}$ , $V_D = V_{DB} = 15\text{ V}$	—	1.90	2.60	$\mu\text{s}$
$t_{off}$	$V_{IN} = 0 \leftrightarrow 5\text{ V}$ , $I_C = 25\text{ A}$	—	2.80	3.80	
$t_{c(on)}$	Inductive load (upper-lower arm)	—	0.60	0.90	
$t_{c(off)}$		—	0.50	0.90	
$t_{tr}$		—	0.60	—	

##### Converter part

Item	Condition	Minimum value	Standard value	Maximum value	Unit
$I_{RRM}$	$V_R = V_{RRM}$ , $T_j = 125^\circ\text{C}$	—	—	7.0	mA
$V_F$	$T_j = 25^\circ\text{C}$ , $I_F = 25\text{ A}$	—	1.1	1.4	V

##### Brake part

Item	Condition	Minimum value	Standard value	Maximum value	Unit	Item
$V_{CE(sat)}$	$V_D = V_{DB} = 15\text{ V}$ , $T_j = 25^\circ\text{C}$	—	1.50	2.20	V	$V_F$
	$V_{IN} = 5\text{ V}$ , $I_C = 15\text{ A}$ , $T_j = 125^\circ\text{C}$	—	1.80	2.45		
$t_{on}$	$T_j = 125^\circ\text{C}$ , $V_{CC} = 600\text{ V}$ , $V_D = V_{DB} = 15\text{ V}$	—	1.10	1.90	$\mu\text{s}$	$t_{c(on)}$
$t_{off}$	$V_{IN} = 0 \leftrightarrow 5\text{ V}$ , $I_C = 15\text{ A}$	—	2.60	3.60		
$t_{c(on)}$	Inductive load	—	0.65	1.00		
$t_{c(off)}$		—	0.40	0.95		
$t_{tr}$		—	0.65	—		

the rated electric current by approx. 18% compared to the conventional large DIPIPM Ver. 4 series. As a typical example, Fig. 7 shows the collector current  $I_C$ -saturated voltage  $V_{CE(sat)}$  characteristics ( $T_j = 125^\circ\text{C}$ ) of the large DIPIPM Ver. 4 PS22A76 (25 A/1,200 V), which is the rated electric current counterpart of the PSS25MC1FT (25 A/1,200 V). Due to the reduction of saturated voltage, the power loss per IGBT element with output current  $I_o = 25\text{ A}$  peak in the DIPIPM+ series has been reduced by approx. 10% compared to the conventional large DIPIPM Ver. 4 series.<sup>1</sup>

<sup>1</sup> Conditions:  $T_j = 125^\circ\text{C}$ ;  $V_{CC} = 600\text{ V}$ ;  $PF = 0.8$ ;  $f_c = 5\text{ kHz}$ ; three-phase sine wave output

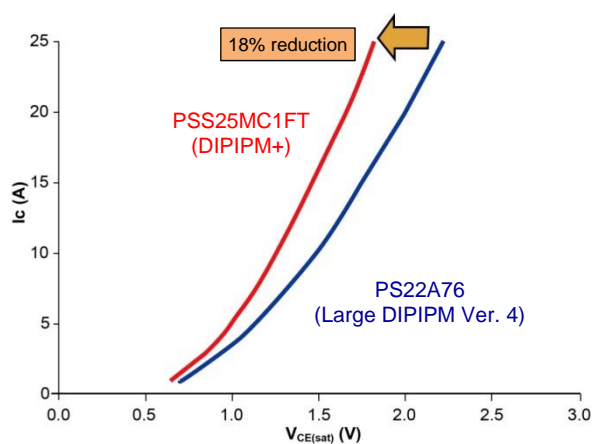


Fig. 7 Collector electric current  $I_C$ -saturated voltage  $V_{CE(sat)}$  characteristics (25-A model)

## 5. Conclusion

This article outlined the functions, features and performance of the new DIPIM+ series launched on the market. We will continue to evolve inverter systems and develop products capable of satisfying a wide variety of market needs.

## References

- (1) Yamaguchi, K., et al.: A New Version Transfer Mold-Type DIPIM™s with built-in Converter and Brake function, PCIM Asia 2015, 272–276 (2015)
- (2) Shiraishi, T., et al.: 1,200 V Large DIPIM “Ver. 4 Series,” Mitsubishi Denki Giho, 84, No. 4, 251–254 (2010).